Acta Scientiarum
http://periodicos.uem.br/ojs
ISSN on-line: 1807-8664
Doi: 10.4025/actascitechnol.v44i1.58823

Daylighting evaluation in deep plan office buildings with OPV windows through simulation on Radiance

Letícia Karine Seki Uehara* **and Aloísio Leoni Schmid**

Programa de Pós-Graduação em Engenharia Civil, Universidade Federal do Paraná, Avenida Coronel Francisco H. dos Santos, 100, 81531-980, Curitiba, Paraná, Brazil. *Author for correspondence. E-mail: leticia.uehara@ufpr.br

ABSTRACT. This research aims to evaluate the OPV window (OPVW) potential application in a deep-plan multi-storey office building, in order to verify its contribution to indoor daylighting quality. OPVW is a cost-effective technology with reduced environmental impact, suitable for application in a multi-story office building due to its potential to adapt to different architectural configurations, lightness and transparency, etc. In an earlier study developed by the authors, an experiment was conducted with a generic office room scale model. Three window materials were compared under real sky conditions (overcast and clear): 3 mm single glass (A scenarios); single glass with OPV (B scenarios); and single glass with application of solar control film (C scenarios). In the present study the same parameters from the experiment were used as input for simulations on Radiance, whose results were compared to previous (work plane illuminance, Daylight Factor and model interior photographs). We found similarities between them. Thus, further results were produced: isolux curves, Daylight Glare Index and render images. The rendered images show a brighter view at A scenarios, and at B and C scenarios. Even if average illuminance is reduced, a better daylight distribution and a reduction in glare are achieved. DGI indicates perceptible glare for some of A scenarios. On the other hand, at most of B and C scenarios, glare was below the perceptible range. Furthermore, the scenarios with OPVW (B scenarios) still show one more advantage: the energy production for artificial lighting when illuminance values are not sufficient.

Keywords: visual performance; computer simulation; isolux curves; Daylight Glare Index; render images.

Received on April 23, 2021.
Accepted on October 25, 2021.

Introduction

Windows play an important role in office building architecture, not only for the aesthetic patterns, but enabling daylight, ventilation and exterior view, as well as biological and physiological benefits to humans. However, without the proper treatment of these surfaces, the occurrence of relevant thermal gains/losses is possible, as well as glare (Hee et al., 2015).

The use of technology to control daylighting in buildings results in lower energy consumption and good visual performance (Sudan, Tiwari, & Al-Helal, 2015). Innovative daylighting systems like Photovoltaic Windows (PVW), apart from electricity production, can reduce energy consumption in terms of cooling, heating and artificial lighting (Skandalos & Karamanis, 2015). Moreover, they allow the improvement of daylighting distribution in deep plan office rooms, in glare control, as well as powering supplementary lighting (Schmid & Uehara, 2017).

Some researchers considered PV suitable for energy generation in Brazil due to the large amount of incident solar radiation there (Cronemberger, Caamaño-Martín, & Sánchez, 2012; Didoné & Wagner, 2013). In Curitiba, the city where the present research was developed, even with the annual global irradiation value of 839 kWh m^{-2} at north façades, smallest in the country, it represents only 6.2% less than the value measured at the south façade in Munich, Germany, where the photovoltaic technology is very widespread (Cronemberger et al., 2012).

Among the different types of photovoltaic windows, one of the emerging technologies, the photovoltaic cells constituted with organic material (OPV) are considered cost-effective with reduced environmental impact (Chemisana et al., 2019). Other OPV advantages are the ease of application in large areas (Skandalos & Karamanis, 2015), the potential of adapting to different architectural configurations, lightness and transparency (Chen et al., 2012). Other advantages are simple architecture, flexibility, color tunability and fast speed and low cost production (Yan, Noble, Peltola, Wicks, & Balasubramanian, 2013). When the OPV

material is replaced by a conventional glass system, it can be used as an UV protection layer (ultraviolet radiation) and NIR (near-infrared radiation), and consequently reduce the cooling load of the building air-conditioning. Thus, in addition to energy savings, the photovoltaic window could convert undesirable radiation into valuable electricity (Yan et al., 2013; Skandalos & Karamanis, 2015).

The general purpose of this study is to evaluate the potential of OPV applied to side windows in deep-plan multi-storey office buildings in order to verify its contribution to the indoor daylighting quality. That means better daylighting distribution and control of excessive brightness (glare) to a worker with direct view to the window. Also, a comparison is made between OPVW and a window with control solar film application for investigating if these two materials have similar behaviors, and provide a means of substantially reducing glare and heat gain without proportionally reducing daylight transmittance. Thus OPV could be a candidate to substitute the solar control film application on windows with an advantage to produce energy for artificial lighting when illuminance values are not sufficient. The specific purpose of this study is to compare previously obtained experimental data with a computer simulation, in order to deepen the understanding of the results.

Material and methods

This research uses an experimental strategy, which was physical in the previously adopted small-scale models, and now numeric, by computer simulation based on the Radiance system. The geometry consists of a single side window placed at the north façade of a deep plan office building. In an earlier study developed by the authors (Uehara, Schmid, Perussi, Pinto, & Oliveira, 2019), a scale model of a generic office room was built and placed on the roof slab of a building at Federal University of Paraná in Curitiba, Brazil (latitude 25º 31 'S and longitude 49º 10' W). Thereafter, three materials types for the side window were evaluated, as shown in Table 1.

The physical scale model made it possible to measure daylighting inside the room under real sky conditions (overcast and clear). The sky condition was identified by a forecast from the Accuweather website, that gives a cloud coverage percentage, and by visual estimation at the measurement time. The results obtained were: work plane (at 75 cm from ground) illuminance along the central axis (north-south); DF (Daylight Factor) for overcast sky; images inside the model for overcast and clear sky conditions. In the present study, these results are further compared with simulation results in order to obtain, work plane illuminance along the central axis; DF (Daylight Factor) for overcast sky; high-quality digital images, a Daylight Glare Index (DGI) calculation.

Daylighting simulation

Daylighting simulation, Radiance was chosen as the lighting simulation program due to its recognition as a well established lighting program that has been used by a number of researchers and could produce a closer prediction to real building measurements than a number of other daylighting simulation programs (Li & Tsang, 2008). Some researchers used Radiance to analyze the daylight performance of a space served by PV windows (Liu, Sun, Wilson, & Wu, 2020; Sun et al., 2020).

Model geometry and materials

The model (Figure 1) corresponds to a generic office room measuring 4.70 (width) x 10.00 (depth) x 3.40 m (height). The depth is aligned with the north-south axis. The room has a side window on the entire north facade (4.70 x 3.40 m). In the present research the same environment, dimensions and characteristics of the physical model previously mentioned were used as input data for the virtual model, in order to compare the measurements made under real sky conditions with the computer simulations. For both, the experiment and the simulation, only daylighting present in the internal environment was considered and no artificial light was used. P1 to P6 indicate the measurement points inside the model, where P1 is the point closest to the window and P6 is the furthest. P6 is also the viewer position used to calculate the Daylight Glare Index (DGI).

Table 1. Scenarios for the simulations.

Scenarios	Materials
Scenario A	3 mm single glass window (90% transmittance)
Scenario B	Same as Scenario A with OPV (2.5% transmittance at the dark bands and 65% transmittance at the bright bands)
Scenario C	Same as Scenario A with solar film application (10% transmittance)

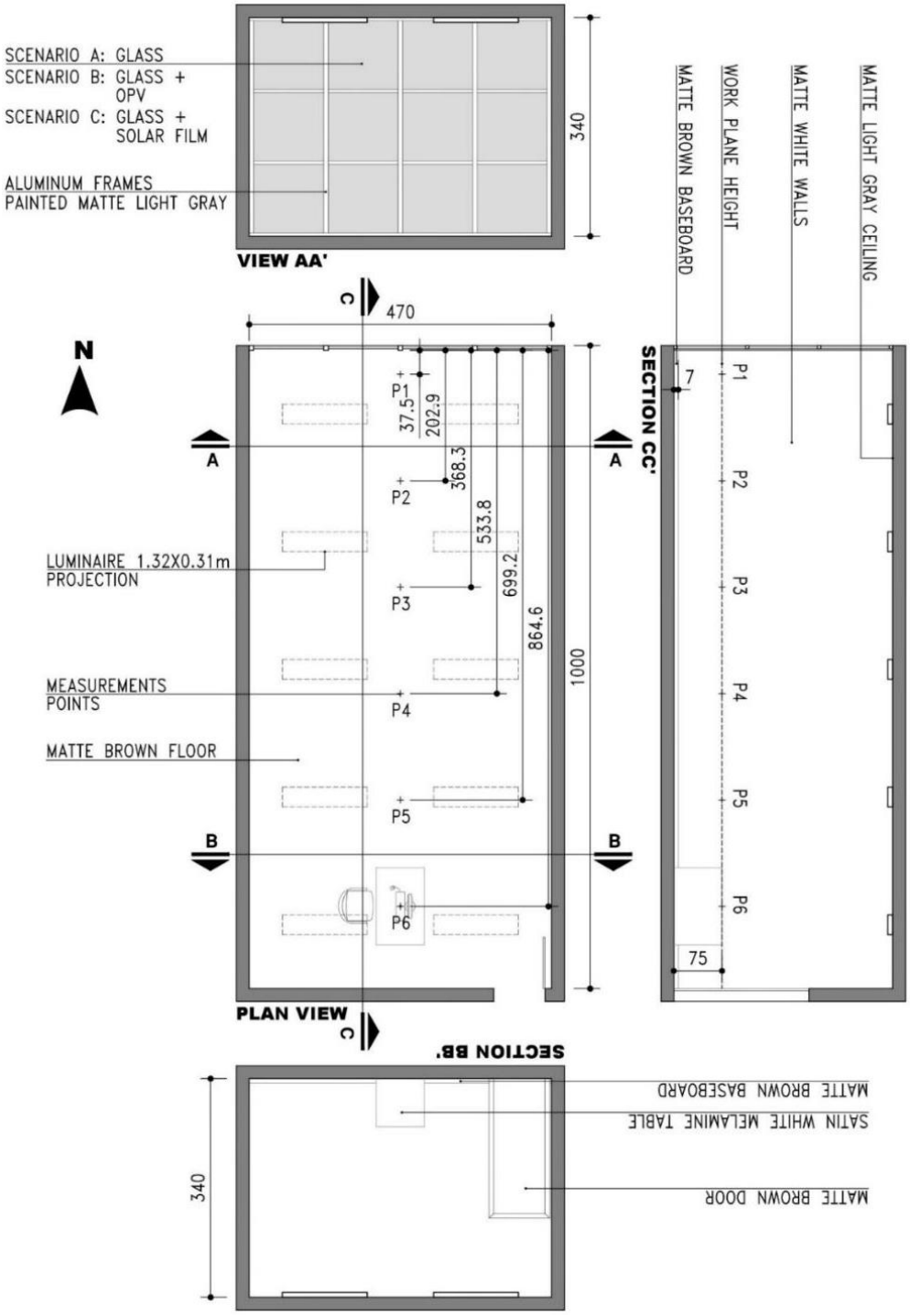

Figure 1. Model geometry for simulations.

Figure 2 shows the location of the model in the environment where the scale model experiment took place in previous research (Uehara et al., 2019). This experiment is used here as input data for the virtual model.

In order to verify if the chosen solar control film could be compared with the photovoltaic module, we submitted the material of scenarios B and C to a UV-VIS test by means of a spectrophotometer (Shimadzu, model NIR2101). This test made it possible to compare the material's transmittance and absorbance by wavelength.

It was observed in the transmittance graph (Figure 3 - left) that the OPV has an advantage over the solar control film, as it allows a greater passage of visible light (400 to 750 nm) and the absorbance graph (Figure 3 - right) shows that both materials behave in a similar way in relation to the absorbed energy, which makes the use of OPV advantageous, as it transforms undesirable radiation into electricity, that can be used for artificial lighting.

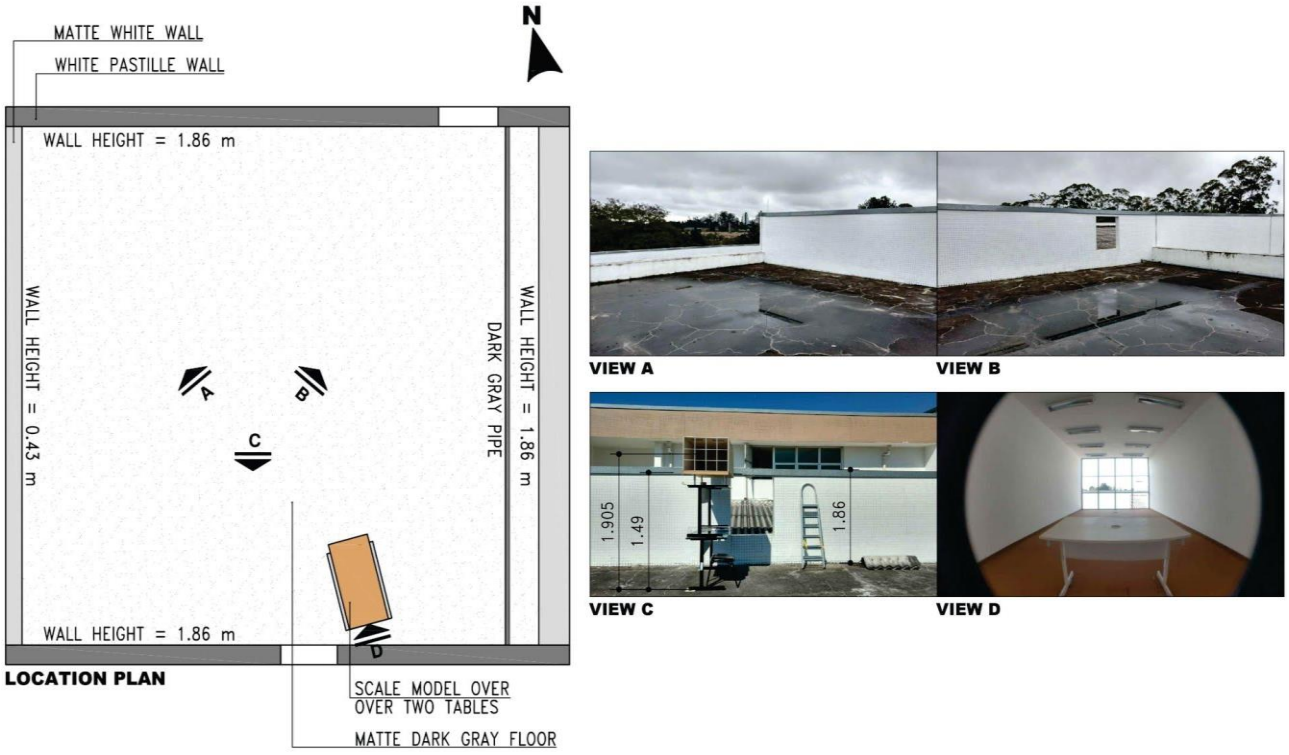

Figure 2. Model location in the environment.

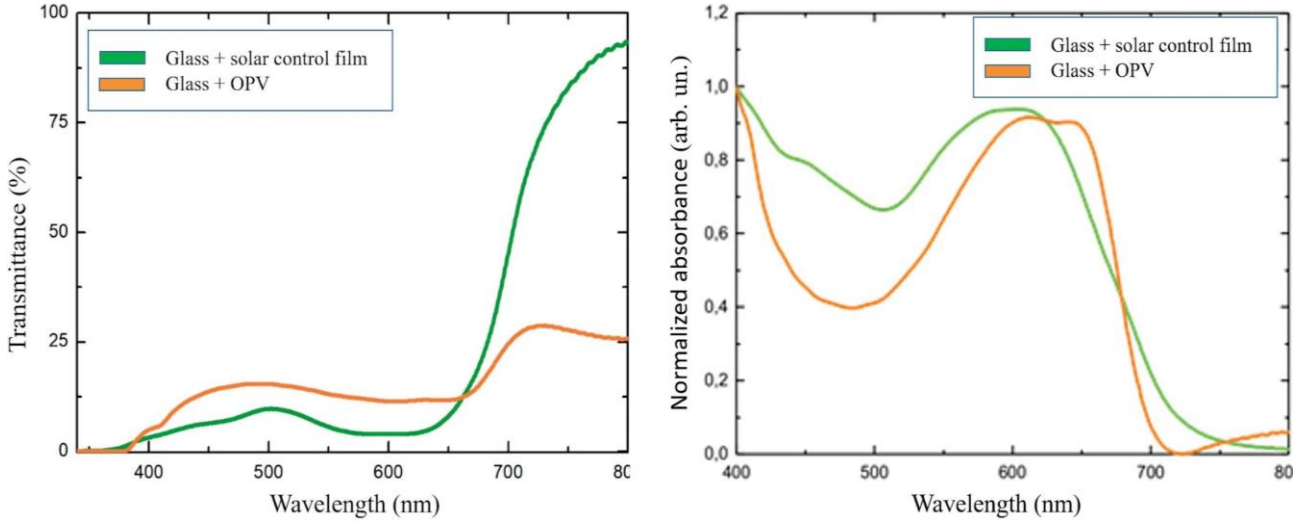

Figure 3. Materials transmittance (left) and Materials absorbance (right).

Data collection

For comparison between the previously obtained scale model measurement and the computer simulation by Radiance, it was necessary to measure the material reflectance. This research uses the surface color estimation method by Larson and Shakespeare (1998). First, small samples of all materials used in the scale model were collected. For color estimation, we used an RGB monitor with adjusted gamma settings and graphic manipulation image package with a color picker: Radiance Colour Picker accessed from the JALOXA website (Jacobs, 2013). This website facilitates the color selection, as it also computes the reflectance and normalized color. The samples were positioned perpendicular to the monitor and the color picker was then adjusted so that the color on the screen resembled the one from the sample. The results obtained using the selected color picker, as shown in Table 2, can be inserted directly into the Radiance input data. Afterwards, the dimensions and characteristics (materials and colors) of the surroundings were surveyed for later insertion of these data into the virtual model.

Table 2. Internal surfaces reflectance.

Surfaces	Material/Radiance material	Color picker reflectance		
		R	G	B
Walls/ceiling	Matte white paint/Plastic	0.95	0.95	0.95
Floor/door/baseboard	Matte brown paint/Plastic	0.38	0.24	0.15
Window 1: Scenario A	Transparent single glass/Glass and illum	0.90	0.90	0.90
Window 2: Scenario B	Transparent single glass/Glass and illum	0.20	0.20	0.20
	Blue transparent glass/Glass and illum	0.18	0.18	0.18
Window 3: Scenario C	Green transparent glass/Glass and illum	0.28	0.33	0.30
Window frames	Matte light gray paint/Plastic	0.19	0.172	0.16
Tables	Satin white paint/Plastic *specularity 0.01	0.691	0.696	0.615
Luminaires (exterior)	Satin white paint/Plastic	0.70	0.60	0.50
Luminaires (interior)	Silver metal/Metal	0.623	0.672	0.692

For measuring the transmittance of the glazing, a simple method with a luxmeter was used. Firstly, the illuminance was measured with the luxmeter above the material, then, another measurement was made with the luxmeter positioned below the material. With this method it was possible to determine the amount of light that passes through the material, in other words, to obtain the transmission value. This procedure was made for all the three types of material (glass, glass with OPV and glass with solar control film). In the OPV case, it was necessary to measure the illuminance in the light and dark ranges of the material. Radiance, in turn, requests transmissivity values. To convert transmittance values to transmissivity, Equation 1 was used, as described by Jacobs (2012):

$$t_n = 1.09T_n \quad (1)$$

where:
t_n is the transmissivity.
T_n is the transmittance.

Work plane illuminance

The method used to calculate the illuminance was described by Jacobs (2012), which uses the rtrace and rcalc tools of Radiance. The first tool calculates the radiance and irradiance values for lighting analysis (Larson & Shakespeare, 1998). In turn, rcalc transforms information from a file according to a set of literal and relational information provided (Radiance, 1999). Data is arranged on the command line as follows:

$ cat data/line.pts | rtrace -I -ab 3 -h -oov scene.oct | rcalc -e '$1=$2;$2=179*(.265*$4+.670*$5+.065*$6)' > results/lux.csv

The input data are the point coordinates (data/line.pts) where measurement has taken place along the room central axis and the scene octree (scene.oct). The result is given in .cvs (results/lux.csv) which can later be accessed in Excel.

Daylight Factor computation

As the external illuminance varies constantly throughout the day, the comparison between the different scenarios was made by means of the Daylight Factor (DF). This metric is expressed as the percentage amount of daylight available inside a room (on a work plane) compared to the amount of unobstructed available daylight outside under overcast sky conditions (Chartered Institution Of Building Services Engineers [CIBSE], 1999). DF values were obtained by the ratio of the luminance values calculated by Radiance to the luminance measured with the luxmeter at an external point of the scale model, as shown in Equation 2:

$$DF = 100\frac{E_{int}}{E_{ext}} \quad (2)$$

where:
E_{int} is internal illuminance;
E_{ext} is external horizontal illuminance under an overcast sky.

According to the practical codes for daylighting BS 6262-2: 2005 and BS 8206-2: 2008, at an average DF value of 5% or more and satisfactory daylight penetration, artificial lighting is not normally required; at an average DF between 2 and 5%, artificial lighting is usually required. When the average DF value is below 2%, artificial lighting is almost always required (Hashemi, 2014). CIBSE (Chartered Institution of Building Services

Engineers) Lighting Guide recommends that DF above 5 does not require complementary artificial light, except at dawn and dusk. However, glare and solar gain may cause problems (CIBSE, 1999).

Render images

The rendered images produced in Radiance had the exposure adjusted so that it was possible to see the scene in its entirety. The normtiff command uses an unfiltered image as input and compresses the dynamic range so that light and dark regions are visible and can be used to mimic certain human visual system features (Jacobs, 2012).

Isolux curves at work plane height

Illuminance was also represented in top views of the room with overlapping isolux curves. The isolux are formed by lines of points on a specified surface where the illuminance has the same value. These images help to understand the daylight distribution in the indoor space.

The method described in the tutorial Radiance Cookbook (Jacobs, 2014) was used to generate the isolux curves. In Radiance, an illuminance image is created on the work plane and then the falsecolor tool uses it to plot the isolux curves on a black background. Afterwards, an adaptation was made in the tutorial method, Photoshop software was used to remove the black background, and the isolux curves were overlapped with an image of the room top view.

Glare computation

Glare is considered the main manifestation of visual discomfort. It occurs when an object that is excessively bright, or brighter than the other object that we want to see, is in our field of view (Hopkinson, Longmore, & Petherbridge, 1980), or in the words of Bian and Luo (2017), glare may be triggered by a high luminance contrast or an inadequate luminance distribution in the observer's field of view.

To predict the degree of glare perception we used a simpler version of the Cornell formula for Daylight Glare Index (DGI), modified by Chauvel, Collins, Dogniaux, and Longmore (1982):

$$DGI = 10log\sum_{i=1}^{m} G_i \quad (3)$$

$$G_i = 0.478\left[\frac{L_s^{16}\Omega_i^{0.8}}{L_b + (0.07\omega^{0.5}L_w)}\right] \quad (4)$$

where:
L_s is the luminance (Cd m^{-2}) of each part of the source;
L_b is the average surface luminance (Cd m^{-2}) in the environment, within the field of view;
L_w is the weighted average background luminance without considering the sources (Cd m^{-2});
ω: solid angle of the sources (ster).

The Radiance ximage tool was used for glare analysis. It allows luminance values to be displayed in a fish-eye image according to the viewer positioned in the deepest region of the room (P6). Then these values were used as input for the equations to obtain the DGI results, which were evaluated using the criterias from Table 3.

Results and discussion

Work plane illuminance

Computer simulations were performed in the Radiance software with input data (day, time and external horizontal illuminance) obtained from the scale model measurements. Measurements were taken at different times throughout the day to verify the daylighting behavior inside the office room. To identify the scenarios, the letter corresponds to the material type used and the number corresponds to the order in which the measurement was performed, the dates and time of each measurement, as well as, sky condition and the illuminance (E) values in lux obtained in Radiance are represented in Table 4 (overcast sky) and 5 (clear sky). Composition of materials types, sky types and measurement hours generated 24 scenarios.

Daylight Factor - DF

As explained before, DF computation is used only for the overcast sky scenarios (A1-A4; B1-B4; and C1-C4), results are presented in Table 6.

Table 3. Degree of glare perception according to DGI.

Classification	Value
Just perceptible	< 18
Perceptible	18-24
Disturbing	24-31
Intolerable	> 31

Source: Adapted from Jakubiec and Reinhart (2012).

Table 4. Work plane illuminance for overcast sky scenarios.

Scenario		A1	B1	C1	A2	B2	C2	A3	B3	C3	A4	B4	C4
Day		06/11/2017			06/11/2017			08/11/2017			08/11/2017		
Hour		14:00			17:30			09:00			12:30		
Illuminance (lux)	E_{P1}	4367	929	633	2751	275	125	4695	541	476	3415	557	597
	E_{P2}	2527	547	366	1590	163	72	2716	318	276	1977	328	345
	E_{P3}	1278	227	185	804	67	37	1376	132	140	1000	135	174
	E_{P4}	755	97	109	477	29	22	810	57	82	592	59	103
	E_{P5}	506	44	73	319	13	14	543	26	55	398	26	69
	E_{P6}	405	22	59	256	7	12	433	13	44	319	14	55

Table 5. Work plane illuminance for clear sky scenarios.

Scenario		A5	B5	C5	A6	B6	C6	A7	B7	C7	A8	B8	C8
Day		12/11/2017			12/11/2017			12/11/2017			13/11/2017		
Hour		13:25			15:30			17:30			13:15		
Illuminance (lux)	E_{P1}	2372	304	323	1550	205	279	2333	124	98	2569	322	266
	E_{P2}	2224	272	231	1587	195	238	1848	111	94	2338	281	251
	E_{P3}	1615	164	172	1193	120	166	1251	67	69	1683	169	183
	E_{P4}	1106	78	116	794	58	112	841	32	47	1142	80	125
	E_{P5}	773	33	84	583	24	82	609	14	34	824	35	89
	E_{P6}	659	16	71	487	11	69	519	7	28	683	16	75

Table 6. Daylight factor for overcast sky scenarios.

Scenario		A1	B1	C1	A2	B2	C2	A3	B3	C3	A4	B4	C4
$E_{ext}(Klux)$		17.9	26.3	22.4	11.3	7.8	4.42	19.3	15.3	16.9	14	15.7	21.1
DF (%)	DF_{P1}	24.4	3.5	2.8	24.3	3.5	2.8	24.4	3.5	2.8	24.4	3.5	2.8
	DF_{P2}	14.1	2.1	1.6	14.1	2.1	1.6	14.1	2.1	1.6	14.1	2.1	1.6
	DF_{P3}	7.1	0.9	0.8	7.1	0.9	0.8	7.1	0.9	0.8	7.1	0.9	0.8
	DF_{P4}	4.2	0.4	0.5	4.2	0.4	0.5	4.2	0.4	0.5	4.2	0.4	0.5
	DF_{P5}	2.8	0.2	0.3	2.8	0.2	0.3	2.8	0.2	0.3	2.8	0.2	0.3
	DF_{P6}	2.3	0.1	0.3	2.3	0.1	0.3	2.3	0.1	0.3	2.3	0.1	0.3
	Average	9.15	1.2	1.05	9.13	1.2	1.05	9.15	1.2	1.05	9.15	1.2	1.05

For all the scenarios the DF values remain approximately constant at all the measurement points. On one hand, the average DF values for A scenarios exceed 5% and have the possibility of causing glare (CIBSE, 1999). On the other hand, a reduction in DF values occurs for scenarios B and C. Even with the possible need for the use of artificial lighting, B and C scenarios do not indicate the possibility of glare.

Figure 4 shows a comparison between the DF values obtained in the previous study (reduced model measurement) and those calculated by Radiance for overcast sky scenarios. It can be observed that the DF values vary from 0.1 (B1-B4) to 24.4% (A1, A3 and A4). The measured and simulated curves in scenarios A (transparent single glass) and C (glass and solar control film) are very close to each other in all graphics. The greatest difference is found at B scenarios (OPV window), where the simulated values at the farthest points from the window (P5 and P6) are underestimated if compared to the experiment with the reduced model. A possible explanation raised at an earlier stage of this research is related to the complexity of describing material from B scenarios (PV window) when modelling in Radiance. The OPV material was represented in Radiance in a simplified fashion using two materials: light-colored stripes (transparent glass) and dark stripes (dark blue glass). The τ/τ_{0° value (ratio of oblique to perpendicular transmissivity of the window material) is lower for scenario B (glass+OPV). This means that the light flux penetrates the room at a low incidence angle and reaches the deep regions is relatively higher than the flux that, at a high incidence angle, reaches the measurement points close to the window.

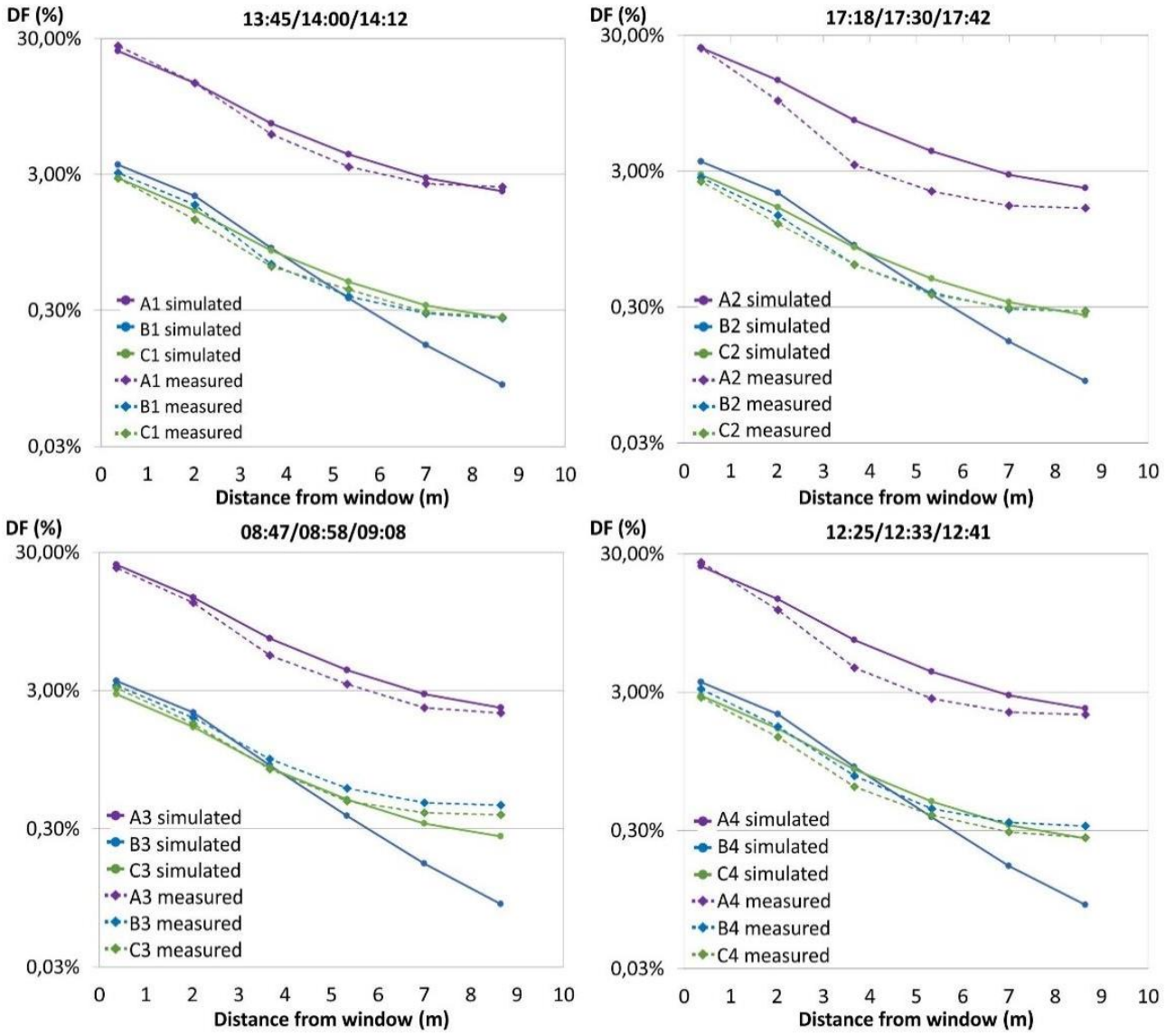

Figure 4. Comparison between simulated and measured DF values under overcast sky.

In the early research, the sky condition was identified by a forecast from the Accuweather website and by a visual estimate. Radiance makes use of the CIE (Commission Internationale de l'Eclairage) sky types, which represent a single and well-defined luminance pattern. Therefore, it was not possible to use the CIE sky standards for overcast sky, as the simulated results became quite discrepant from the measurement in the reduced model. However, with the insertion of measurement data (diffuse horizontal irradiance for overcast sky), the measured and simulated results were closer, and could be validated.

Modelling of the sky luminance distribution is another possible explanation for the discrepant behavior. If the measurement is performed under a sky that is brighter close to the horizon, more radiation will be available to the deeper regions of the room. That effect would cause an even better performance at the B scenario at deep regions. The discrepancy of the DF for OPV, observed at the more distant points from the window, are explained by two hypotheses a) of real transmissivity of glass+OPV varying (more than assumed in simulations) along with obliquity b) of real sky being brighter close to the horizon (than assumed in the simulations). Those hypotheses remain to be tested.

Render images

First, according to Figure 5, six images from the computer simulation (A1, B1, C1, A5, B5 and C5) were selected and compared to corresponding reduced model images (A1*, B1*, C1*, A5*, B5* and C5*). These images were obtained by a smartphone camera (model Z Play, from Motorola) in order to verify the computer simulation capacity to yield realistic results.

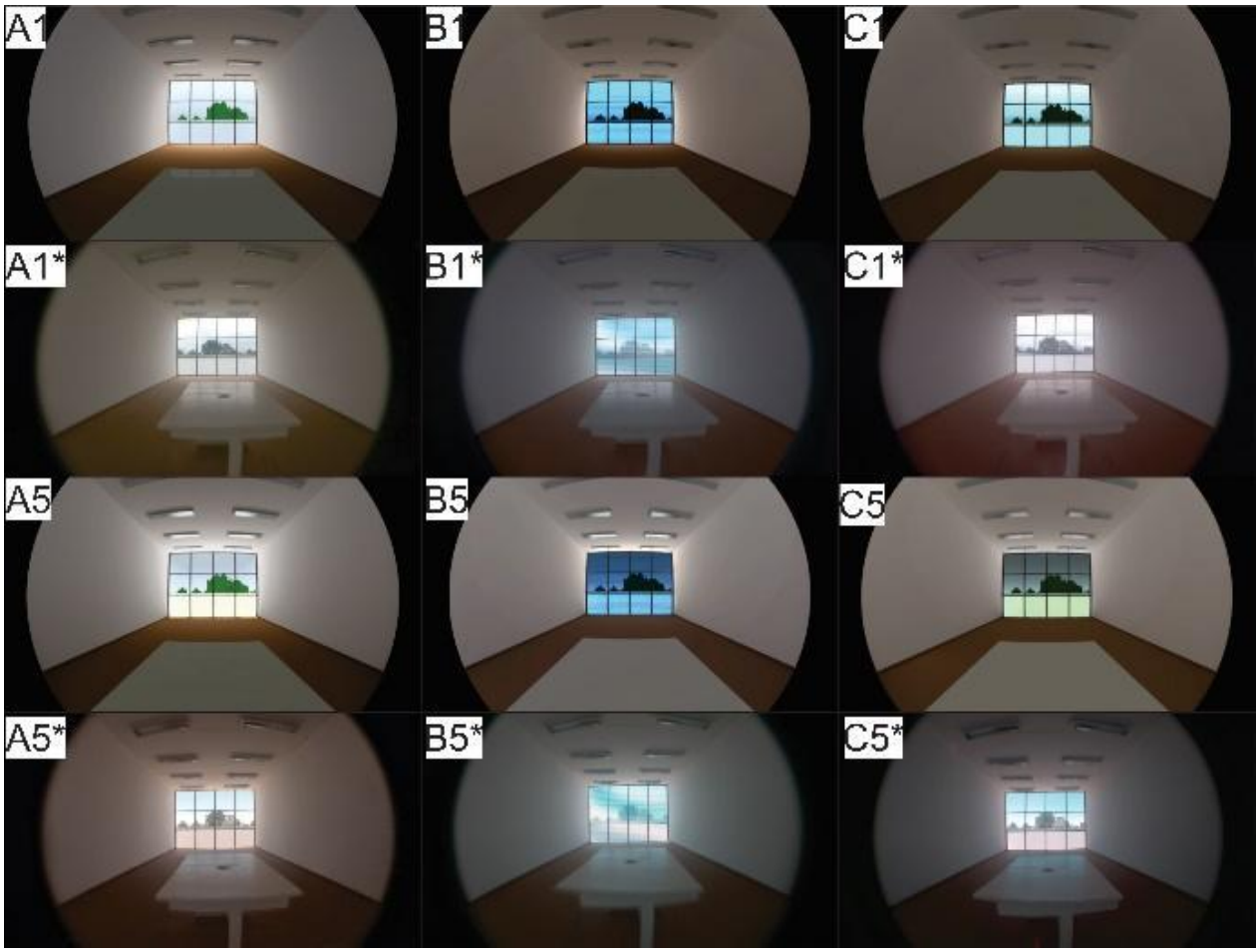

Figure 5. Comparison between computer simulation and reduced model scenarios (last are signaled with *).

One observes that photos are close to Radiance images regarding the daylight behavior. Although the camera HDR images have lost quality due to the lack of a tripod, the reduced model images and the virtual model images show a high resemblance. The most noticeable difference is in the window material color, which seems more saturated in Radiance for the B (close to a solid blue) and C (greenish) scenarios, whereas the reduced model photography shows only a slight color difference regarding the transparent glass window.

Next, Radiance images (Figure 6) were generated for the different scenarios in fish-eye view, as viewed by an observer sitting at the room extremity (opposite to the window). As overcast sky scenarios present only a few subtle differences between the images, only three scenarios (A1, B1 and C1) were represented. On the other hand, clear sky scenarios show rather noticeable differences, so all scenarios under that sky condition (A4 to A8; B4 to B8 and C4 to C8) were represented.

The normtiff tool was used to enable all areas of the scene to be visible in the Radiance rendered images. Therefore, one should not analyze the scene illuminance, but the daylight distribution. In the transparent glass scenarios (A1 to A8) an intense brightness originating from the light source (window) could be observed. However, a small amount of daylight reaches the deepest areas of the room. This may cause glare due to the high contrast between the window and the areas close to the table where the observer is.

Due to the use of the normtiff tool, the other scenarios (B1 to B8 and C1 to C8) seem to show more daylight than the transparent glass scenarios (A1 to A8). This happens because the tool has to increase exposition at B and C scenarios in order to make all of the scene areas visible, while in transparent glass scenarios such increase is not necessary. Moreover, B and C scenarios present a reduction in the window brightness and therefore a smaller contrast. Even if there is also a reduction in the luminous flux that passes through the window at B and C scenarios, this is explained by an improvement in the daylight distribution.

Isolux curves

Isolux curves are shown over room plans on Figure 7 at left for overcast (2, 3 and 4) and at right for clear (5, 6 and 7) skies. As the illuminance values for the transparent glass scenarios under overcast sky presented

higher values than the other scenarios, a scale of 0 to 5,000 lux was adopted. For clear sky the scale ranges from 0 to 2,500 lux. The A scenarios only illustrate the light flux entering the room in the case of transparent glass, which is quite higher compared to the other scenarios.

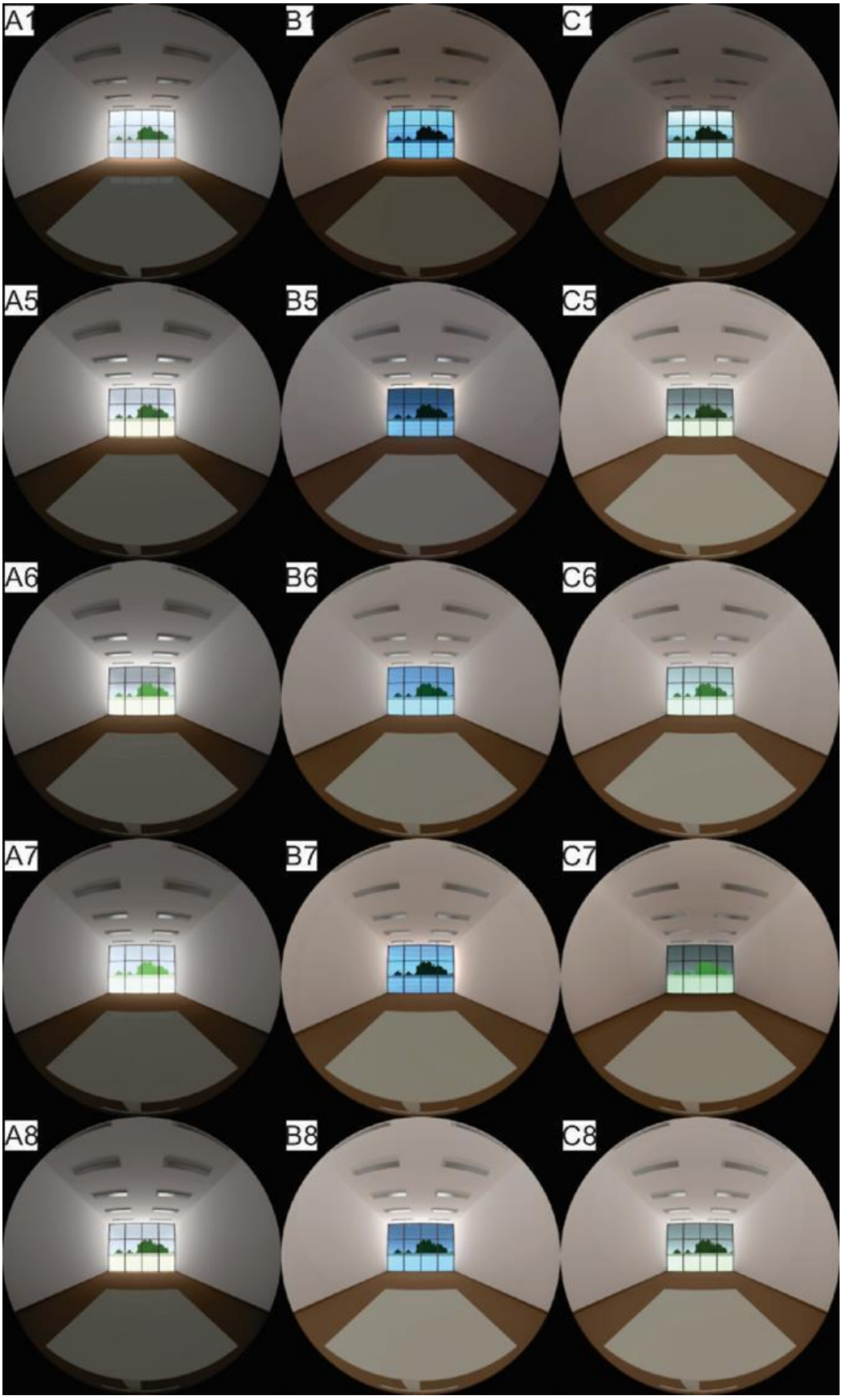

Figure 6. Window view of an observer sitting on the back of the room for the overcast and clear sky scenarios.

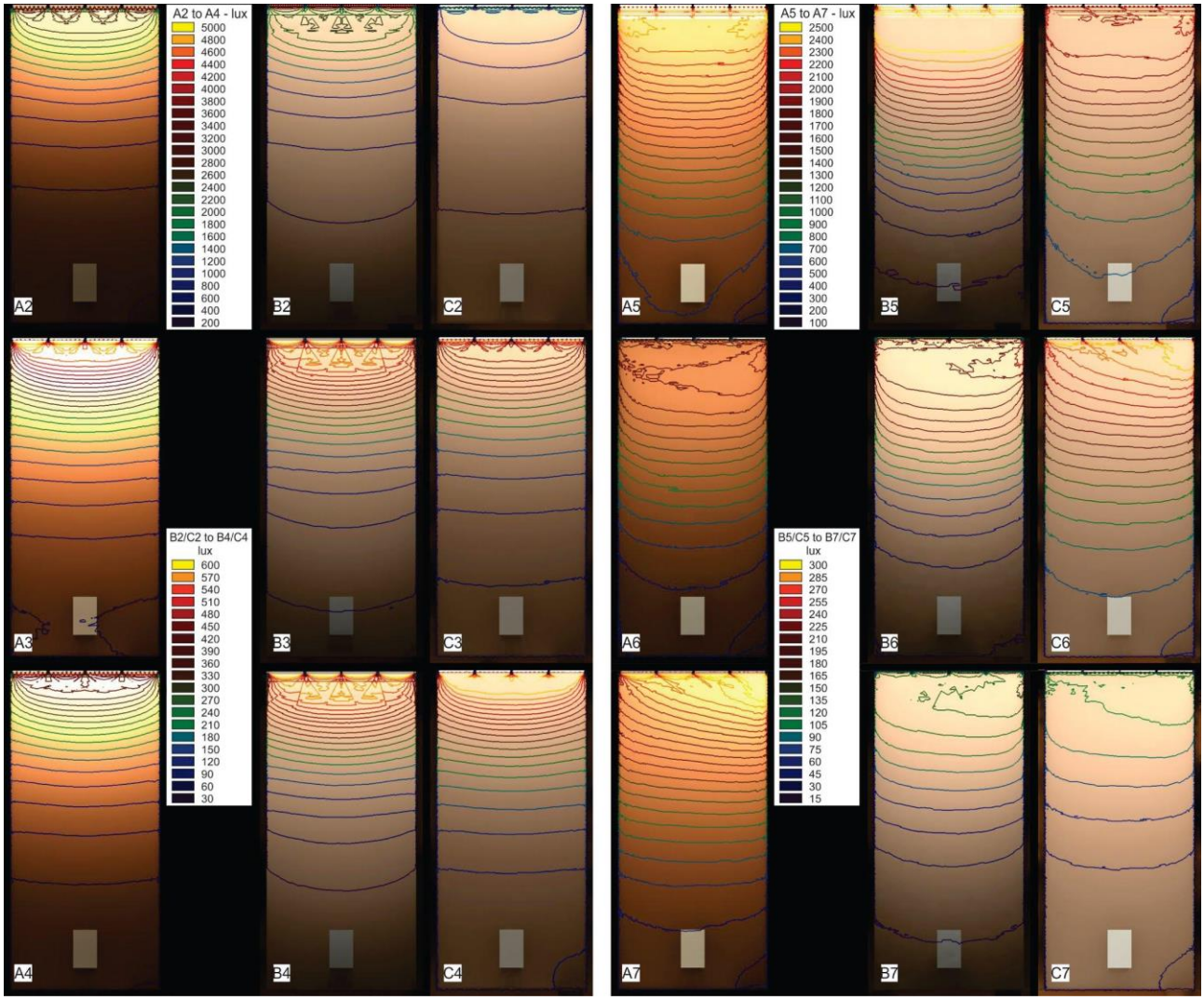

Figure 7. Top view with isolux curves for overcast sky scenarios (at left) and top view with isolux curves for clear sky scenarios (at right).

As B and C scenarios have equivalent average window transmittance, it was possible to use the same range to compare them: 0 to 600 lux for overcast sky, and 0 to 300 lux for clear sky. Isolux curves at B and C scenarios show higher values at C than at B, as daylight reaches deeper regions in the room. However, this data contradicts the findings in the former study, where the OPV window was shown to allow more light to reach the deepest areas of the room. This situation occurs only at the farthest points from the window (P5 and P6). As in the former study a reduced model was examined under real sky conditions, those findings are held as valid.

Even if the A scenarios have yielded highest DF values, it does not mean a higher lighting quality. As daylight is not distributed in an adequate fashion, it creates a higher contrast between the areas close to the window and the areas at deep regions of the room. This may cause glare to the room users. On the other hand, at B and C scenarios, average illuminance values are lower, however its distribution is more even, with a lower contrast. Comparing these two scenarios, B could show an advantage over C, because the OPV cells can produce energy for artificial lighting, when adequate illuminance values are not reached.

Glare

Glare was calculated and expressed as Daylight Glare Index (DGI). First, the ximage tool in Radiance was applied to generate a fish-eye image for each scenario. This tool allows us to find the average luminance for each surface and source. Data were inserted into the DGI formula and results under overcast sky are shown at Table 7, and for clear sky at Table 8.

Table 7. DGI for overcast sky scenarios.

Scenarios	A1	B1	C1	A2	B2	C2	A3	B3	C3	A4	B4	C4
L_s	1562	608	217	1001	134	110	1681	258	396	1232	286	498
L_s	526	379	71	348	208	192	558	256	281	419	264	312
L_s	172	301	109	125	233	220	174	256	242	142	257	248
DGI	22	17	15	21	9	7	22	12	15	21	13	16

Table 8. DGI for clear sky scenarios.

Scenarios	A5	B5	C5	A6	B6	C6	A7	B7	C7	A8	B8	C8
L_s	2322	211	288	4665	600	801	9861	235	886	3156	259	323
L_s	1118	272	270	1625	373	396	2959	260	388	1334	285	280
L_s	707	293	263	586	296	258	601	268	218	711	294	266
DGI	21	11	13	25	17	18	27	12	19	23	12	13

The transparent glass scenarios (A1, A2, A3, A4, A5 and A8) presented highest DGI values ranging from 21 to 23 and are at the perceptible range. At clear sky scenarios A6 and A7, DGI values of 25 and 27, respectively, were found. In such a range glare is considered disturbing and countermeasures are needed.

In other scenarios, with OPV (B) and glass with solar control film (C), under both overcast and clear sky, almost all glare values were below the perception threshold. C7 showed a DGI value of 18 (perceptible). In addition, there was a similarity between DGI values at B and C, suggesting that both materials are of comparable performance regarding glare control.

Conclusion

OPV window potential application in a deep-plan office building was evaluated by comparing three materials types for the window (3 mm single glass – A scenarios; single glass with OPV – B scenarios; and single glass with application of solar control film – C scenarios). Results showed that although the A scenarios presents higher illuminance values, in the B and C scenarios, even with the possible need for the use of artificial lighting, a better daylight distribution and a reduction in glare are achieved. Furthermore, OPVW scenarios present the advantage of energy production for artificial lighting when illuminance values are not sufficient.

Acknowledgements

We would like to thank the SUNEW company for the loan of the OPV photovoltaic module for the experiment; Professor Lucimara Stolz Roman and the students of the Laboratory of NanoStructured Devices (DiNE) at UFPR for their help throughout the experiment and especially for the production of absorbance and transmittance graphs; and, to the support of the Graduate Program in Civil Engineering (PPGEC) of UFPR.

References

Bian, Y., & Luo, T. (2017). Investigation of visual comfort metrics from subjective responses in China: a study in offices with daylight. *Building and Environment, 123*, 661-671. DOI: https://doi.org/10.1016/j.buildenv.2017.07.035

Chartered Institution Of Building Services Engineers [CIBSE]. (1999). *Lighting guide LG10: daylighting and window design*. London, GB: CIBSE.

Chauvel, P., Collins, J. B., Dogniaux, R., & Longmore, J. (1982). Glare from windows: current views of the problem. *Lighting Research & Technology, 14*(1), 31-46. DOI: https://doi.org/10.1177/096032718201400103

Chemisana, D., Moreno, A., Polo M., Aranda, C., Riverola, A., Ortega, E., ... Cot, A. (2019). Performance and stability of semitransparent OPVs for building integration: A benchmarking analysis. *Renewable Energy, 137*, 177-188. DOI: https://doi.org/10.1016/j.renene.2018.03.073

Chen, K.-S., Salinas, J.-F., Yip, H.-L., Huo, L., Hou, J., & Jen, A. K.-Y. (2012). Semi-Transparent polymer solar cells with 6% PCE, 25% average visible transmittance and a color rendering index close to 100 for power generating window applications. *Energy & Environmental Science, 5*(11), 9551-9557. DOI: https://doi.org/10.1039/c2ee22623e

Cronemberger, J., Caamaño-Martín, E., & Sánchez, S. V. (2012). Assessing the solar irradiation potential for solar photovoltaic applications in buildings at low latitudes – Making the case for Brazil. *Energy and Buildings, 55*, 264-272. DOI: https://doi.org/10.1016/j.enbuild.2012.08.044

Didoné, E. L., & Wagner, A. (2013). Semi-transparent PV windows: a study for office buildings in Brazil. *Energy and Buildings, 67*, 136-142. DOI: https://doi.org/10.1016/j.enbuild.2013.08.002

Hashemi, A. (2014). Daylighting and solar shading performances of an innovative automated reflective louvre system. *Energy and Buildings, 82*, 607-620. DOI: https://doi.org/10.1016/j.enbuild.2014.07.086

Hee, W. J., Alghoul, M. A., Bakhtyar, B., Elayeb, O., Shameri, M. A., Alrubaih, M. S., & Sopian, K. (2015). The role of window glazing on daylighting and energy saving in buildings. *Renewable and Sustainable Energy Reviews, 42*, 323-343. DOI: https://doi.org/10.1016/j.rser.2014.09.020

Hopkinson, R. G., Longmore, J., & Petherbridge, P. (1980). *Iluminação natural*. Lisboa, PT: Fundação Calouste Gulbenkian.

Jacobs, A. (2012). *Radiance tutorial*. Retrieved from http://www.jaloxa.eu/resources/radiance/documentation/docs/radiance_tutorial.pdf

Jacobs, A. (2013). *Radiance colour picker*. Retrieved from http://www.jaloxa.eu/resources/radiance/colour_picker.shtml

Jacobs, A. (2014). *Radiance cookbook*. Retrieved from http://www.jaloxa.eu/resources/radiance/documentation/docs/radiance_cookbook.pdf

Jakubiec, J. A., & Reinhart, C. F. (2012). The 'adaptive zone' - A concept for assessing discomfort glare throughout daylit spaces. *Lighting Research & Technology, 44*(2), 149-170. DOI: https://doi.org/10.1177/1477153511420097

Larson, G. W., & Shakespeare, R. (1998). *Rendering with RADIANCE: art and science of lighting visualization*. San Francisco, CA: Morgan Kaufmann.

Li, D. H. W., & Tsang, E. K. W. (2008). An analysis of daylighting performance for office buildings in Hong Kong. *Building and Environment, 43*(9), 1446-1458. DOI: https://doi.org/10.1016/j.buildenv.2007.07.002

Liu, D., Sun, Y., Wilson, R., & Wu, Y. (2020). Comprehensive evaluation of window-integrated semi-transparent PV for building daylight performance. *Renewable Energy, 145*, 1399-1411. DOI: https://doi.org/10.1016/j.renene.2019.04.167

Radiance. (1999). *Manual pages*. Retrieved from https://www.radiance-online.org/learning/documentation/manual-pages/pdfs/rcalc.pdf

Schmid, A. L., & Uehara, L. K. S. (2017). Lighting performance of multifunctional PV windows: a numeric simulation to explain illuminance distribution and glare control in offices. *Energy and Buildings, 154*, 590-605. DOI: https://doi.org/10.1016/j.enbuild.2017.08.040

Skandalos, N., & Karamanis, D. (2015). PV glazing technologies. *Renewable and Sustainable Energy Reviews, 49*, 306-322. DOI: https://doi.org/10.1016/j.rser.2015.04.145

Sudan, M., Tiwari, G. N., & Al-Helal, I. M. (2015). A daylight factor model under clear sky conditions for building: an experimental validation. *Solar Energy, 115*, 379-389. DOI: https://doi.org/10.1016/j.solener.2015.03.002

Sun, Y., Liu, D., Flor, J.-F., Shank, K., Baig, H., Wilson, R., ... Wu, Y. (2020). Analysis of the daylight performance of window integrated photovoltaics systems. *Renewable Energy, 145*, 153-163. DOI: https://doi.org/10.1016/j.renene.2019.05.061

Uehara, L. K. S., Schmid, A. L., Perussi, M., Pinto, V. H. S., & Oliveira, M. (2019). Avaliação do potencial da janela OPV para iluminação natural de salas profundas. *PARC Pesquisa em Arquitetura e Construção, 10*, e019004. DOI: https://doi.org/10.20396/parc.v10i0.8652752

Yan, F., Noble, J., Peltola, J., Wicks, S., & Balasubramanian, S. (2013). Semitransparent OPV modules pass environmental chamber test requirements. *Solar Energy Materials and Solar Cells, 114*, 214-218. DOI: https://doi.org/10.1016/j.solmat.2012.09.031